Solid Freeform Fabrication 2017: Proceedings of the 28th Annual International Solid Freeform Fabrication Symposium – An Additive Manufacturing Conference
Reviewed Paper

BINDER JET ADDITIVE MANUFACTURING OF STAINLESS STEEL - TRICALCIUM PHOSPHATE BIOCOMPOSITE FOR BONE SCAFFOLD AND IMPLANT APPLICATIONS

Kuldeep Agarwal, Sairam Vangapally and Alexander Sheldon

Department of Automotive and Manufacturing Engineering Technology, Minnesota State University, Mankato, 56001

Abstract

Scaffolds are 3D biocompatible structures that mimic the extracellular matrix properties (mechanical support, cellular activity and protein production) of bones and provide place for cell attachment and bone tissue formation. Their performance depends on chemistry, pore size, pore volume, and mechanical strength. Recently, additive manufacturing (AM) has been used as a means to produce these scaffolds. This paper explores a new biocomposite manufactured using Binder Jet AM process. Stainless steel and tricalcium phosphate are combined to form a composite and used in different volume fractions to produce parts with varying densities. Layer thickness, sintering time and sintering temperature are varied to study the effect of process parameters on the microstructure, dimensions and mechanical properties of the resulting structure. It is found that the resulting biocomposite can be tailored by varying the process to change its properties and mimic the properties of scaffolds in bone tissue applications.

Introduction

Biomedical implants can be classified into 3 major categories: external to the body (non-clinical, which includes surgical instruments, prosthetics etc.), internal to the body & permanent (includes hip implants, knee implants, stents etc.), and internal to the body & temporary (includes scaffolds, degradable screws and drug delivery systems) [1-3, 14].

According to FDA, a ‘‘permanently implantable device is a device that is intended to be placed into a surgically or naturally formed cavity of the human body for more than one year to continuously assist, restore, or replace the function of an organ system or structure of the human body throughout the useful life of the device.’’ Some examples include knee and hip implants. Temporary implants are commonly used in sports surgeries, such as in shoulder and knee ligamentous reconstruction and spinal reconstructive surgery [5, 6, 14].

Scaffolds are temporary porous structures implanted to assist in tissue or bone regeneration. They are three-dimensional structures that mimic the extracellular matrix (ECM) properties (mechanical support, cellular activity, and protein production) and provide place for cell attachment and bone tissue formation. "The performance of scaffolds" depends on chemistry, pore size, pore volume and mechanical strength. Interconnected porosity is important for continuous ingrowth of bone tissue. Open and interconnected pores allow nutrients and molecules to transport to inner parts of the scaffold. An ideal scaffold must satisfy the following requirements:

- Biocompatibility
- Biodegradability
- Appropriate porosity, pore size and pore shape
- Bioactive
- Mechanical strength
- Adequate surface finish
- Easily manufactured and sterilized

The most common biomaterials for implants are metals and alloys, ceramics, and polymers. Among the metals, one of the most important classes of materials due to its corrosion resistance is stainless steel. Bones have elastic moduli 7 - 30 GPa, yield stress 30 - 70 MPa, compressive strength 100 - 230 MPa, and tensile strength 70 - 150 MPa. The first generation of implants focused on replacement of the bone with a metal implant. However, mechanical properties of metals differ considerably from natural bone: Stainless steel elastic modulus = 190 GPa, yield strength = 220 - 1213 MPa, tensile strength 586 - 1352 MPa [3, 4, 7].

These differences lead to stress shielding resulting in loosening of the implant due to degradation of human tissues around implants and, consequently, further surgeries to replace the implants. Ceramics are inorganic materials with high compressive strength and biological inertness that make them suitable for scaffolds used in strengthening or replacing damaged bones and tissues. The most commonly used bioceramics are metallic oxides (e.g., Al_2O_3, MgO), calcium phosphate (e.g., hydroxyapatite (HA), tricalcium phosphate (TCP), and octacalcium phosphate (OCP)), and glass ceramics (e.g. Bioglass, Ceravital).

Calcium phosphates have the best biocompatibility and properties closest to natural bones: elastic modulus 7 -13 GPa, compressive strength 350 - 450 MPa, tensile strength 38 - 48 MPa and flexural strength 100 - 120 MPa. However, they have poor fracture toughness and tensile strength that limits their application to bioimplants. Several in vitro and vivo works have shown that calcium phosphates support the adhesion, differentiation, and proliferation of osseogenesis-related cells (e.g., osteoblasts, mesenchymal stem cells), besides inducing gene expression in bone cells. The most important calcium phosphate is hydroxyapatite (HA, $Ca_{10}(PO_4)_6(OH)_2$) with chemical characteristics similar to hard tissues such as bone and teeth, that promotes hard tissue ingrowth and osseointegration when implanted into the human body. The porous structure of this material can be tailored to suit the interfacial surfaces of the implant. As a bulk material, HA lacks sufficient tensile strength and is too brittle to be used in most load bearing applications. In such cases, HA is coated onto a metal core or incorporated into polymers as composites. The ceramic coating on the titanium implants improves the surface bioactivity but often fails as a result of poor ceramic/metal interface bonding [8-11].

α-TCP and β-TCP are the two crystalline varieties of HA of interest in biological applications. β-TCP is the thermodynamically stable form at low temperature. It transforms into **α**-TCP in the temperature range 1120 - 1170 ºC. β-TCP is generally preferred in sintered ceramic implants, while **α**-TCP is more commonly used in bone graft cements because of its hydrolysis properties. The requirements that allow bone ingrowth are a porosity of 30 - 70 vol % and a pore diameter between 300 and 800 µm, mechanical properties of 0.5 - 15 MPa similar to cancellous bone.

Thus there is a drive in the biomedical industry to create novel materials that behave very similar to bone and can be used for multiple applications: from permanent to temporary implants. Furthermore, these materials need to be manufactured in a manner that would create porosity in situ for biological applications. The current techniques used for making scaffolds are salt leaching, gas forming, phase separation, freeze-drying.

Due to the versatility of additive manufacturing, it is gaining a lot of popularity in the field of bone implants. Selective Laser Sintering, Selective Laser Melting, Electron Beam Melting and Binder jet manufacturing have all been used to create various porous structures for biomedical implants [7, 9]. To accomplish the various different requirements of the implants it is necessary to create biocomposites that can have the strength properties of metals as well as the biological properties of bioceramics.

The present work aims at creating such structures by manufacturing and studying a stainless steel (SS) – Tricalcium phosphate (TCP) biocomposite with binder jet AM process. In this work SS and TCP are combined to form a composite and used in different volume fractions to produce parts with varying densities. Layer Thickness, Sintering time and Sintering temperature are varied to study the effect of process parameters on the microstructure, dimensions and mechanical properties of the resulting structure.

Binder Jet-based Additive Manufacturing

The main technique of manufacturing using the binder jet process is as follows: (a) the CAD file is sliced into layers and a STL file is generated, (b) each layer begins with a thin distribution of powder spread over the surface of a powder bed, (c) using a technology similar to ink-jet printing, a binder material selectively joins particles where the object is to be formed, (d) a piston that supports the powder bed and the part-in-progress lowers so that the next powder layer can be spread and selectively joined, (e) this layer-by-layer process repeats until the part is completed, (f) following a heat treatment, unbound powder is removed and the metal powder is sintered together. Fig. 1 shows the details of the whole process.

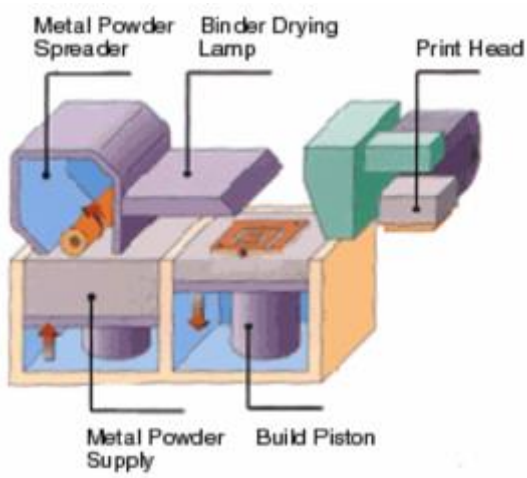

Fig. 1: Schematic of the Binder Jet Process (Courtesy The ExOne Company)

Process parameters

The binder jet process described above can be divided into 3 basic steps: 1) binding, 2) curing and 3) sintering. There are various process parameters that can be changed to obtain a customized part in each of these steps. These include powder size, layer thickness during binding, part orientation in bed, heater power, roller speed, curing temperature, curing time, sintering time, sintering temperature, and sintering atmosphere. To study the effect of each of these parameters and their interactions would require a huge experimental design and many hundreds of samples and testing. A feasibility study was done to see if a biocomposite can be created using this manufacturing technique where only the volume fraction of TCP, layer thickness, sintering time, and temperature were varied.

Experimental Plan

The materials used in the study were stainless steel 316 (SS316), which has a mean particle size of 30μm and an apparent density of 2.75 g/cc. The chemical composition of SS316 is shown in Table 1.

C	Mn	P	S	Si	Cr	Ni	Mo
0.08 max	2.0 max	0.045 max	0.03 max	0.75 max	16.0 - 18.0	10.0 – 14.0	2.0 – 3.0

Table 1: Chemical composition of SS316 (wt %)

β-TCP was obtained from Sigma-Aldrich (21218) with a mean particle size of 5μm and an apparent density of 1.92 g/cc. Scanning Electron Microscope (JEOL JSM-6510MV) was used to look at the sizes and distribution of the powders before the process. The images are shown in Fig. 6.

SS316 was used as a benchmark and is called Sample Set 1. The two powders were mixed in 2 different volume fractions: Sample set 2 with 80% SS316-20% TCP and sample set 3 with 60% SS316-40% TCP. The mixed powders and the SEM images are shown in Fig. 2 and 3, respectively.

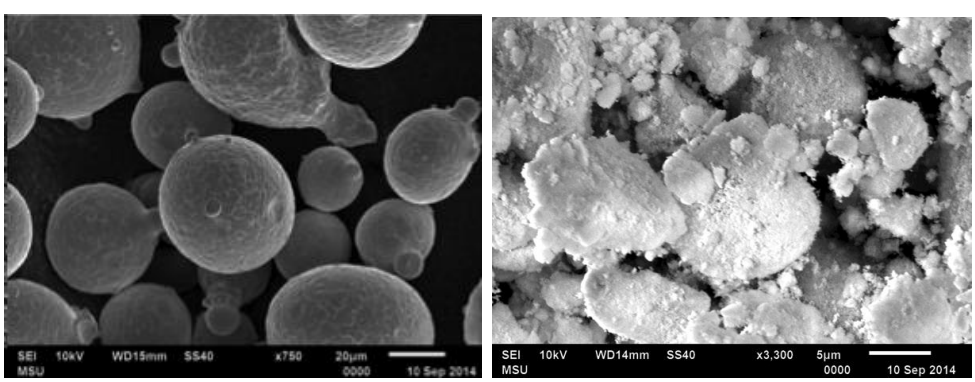

Fig. 2: SEM Micrographs for SS316 and TCP

The 3 sample sets were then used as the input powders in the binder jet additive manufacturing. To understand the effect of process parameters of the binder jet process on the material properties, 2 different layer thicknesses were chosen: 50 µm and 100 µm. The sintering time was varied as 2 hours and 4 hours and the sintering temperature as 1100 ^{o}C and 1200 ^{o}C. The design of experimental matrix is shown in Table 2. Three replicates of each experiment were done.

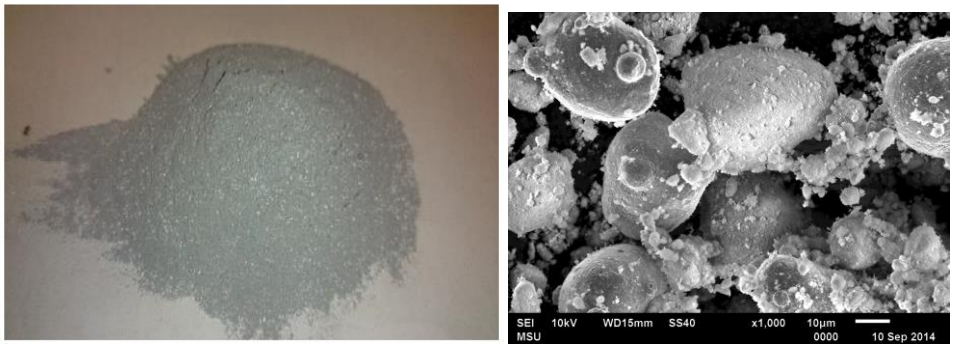

Fig. 3: Mixed sample set 1 of SS316-TCP (left) and the SEM image (right)

Expt No.	% TCP	Layer Thickness (µm)	Sintering Time (Hrs)	Sintering Temp (^{0}C)
1	0	50	2	1100
2	0	50	2	1200
3	0	50	4	1100
4	0	50	4	1200
5	0	100	2	1100
6	0	100	2	1200
7	0	100	4	1100
8	0	100	4	1200
9	20	50	2	1100
10	20	50	2	1200
11	20	50	4	1100
12	20	50	4	1200
13	20	100	2	1100
14	20	100	2	1200
15	20	100	4	1100
16	20	100	4	1200
17	40	50	2	1100
18	40	50	2	1200
19	40	50	4	1100
20	40	50	4	1200
21	40	100	2	1100
22	40	100	2	1200
23	40	100	4	1100
24	40	100	4	1200

Table 2: Design of Experimental Matrix

Printing, Curing and Sintering.

Samples were printed based on ASTM E9 specification for compression testing. Three samples from each set were printed for compression testing. The roller speeds were kept at the minimum of 1 mm/sec. The samples were cylinders with diameter of 12.5 mm and height of 22.5 mm.

After printing the samples were cured in an oven at 175^0C for 3 hours. The cured parts were sintered in an Ar atmosphere. After sintering the samples were removed and cleaned. The samples at each stage are shown in Fig. 4.

Fig. 4: Samples while being printed and after the sintering and after machining

Experiments: Compression testing

The samples were tested according to ASTM E9 standards [10]. The samples were setup for compression testing on the MTS 810 material testing system. The MTS machine was set to run failure detect mode test at speeds of 15 mm/min. The stress strain curves were then calculated for all the experiments. The sample in the machine for testing and the crushed sample after testing are shown in Fig. 5.

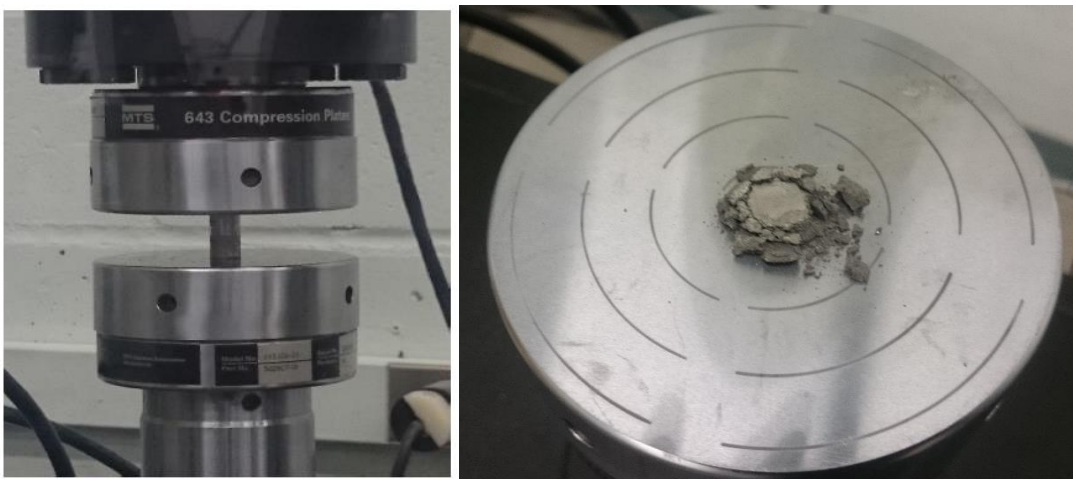

Fig. 5: Compression testing

Microstructural Analysis

Scanning electron microscope was used to study the microstructure of samples before and after sintering. The images were used to calculate the neck to diameter ratio for each sample

$$\text{Neck size ratio} = \frac{x}{D}$$

Where, x is neck diameter and D is particle diameter. Ten different measurements were taken from different images of the sample and they were averaged. The images were also used to calculate the pore sizes. The behavior of TCP and its interaction with SS316 was also studied [12, 13, 14].

Results

SEM Analysis

The sintered SS316-TCP biocomposites were examined under a SEM. The resulting structures are shown in Fig. 11 with both the constituents.

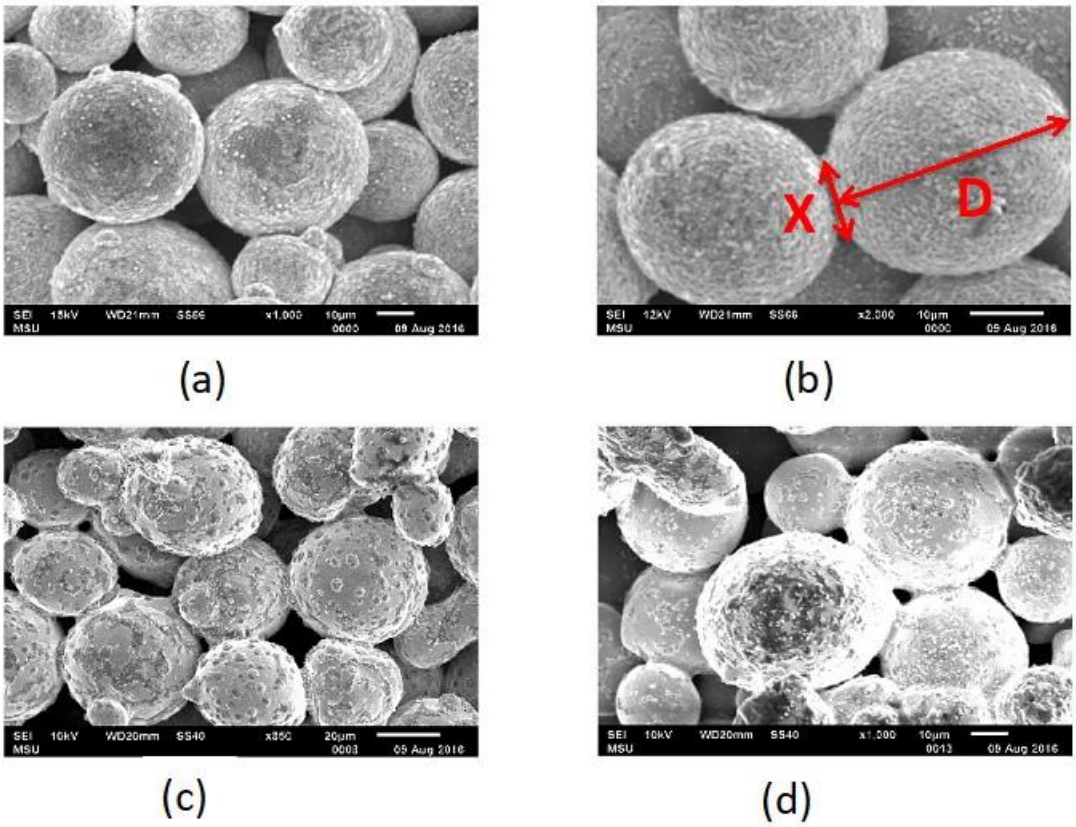

Fig. 6: SEM Images of (a) Expt 1 (b) Expt 2 (c) Expt 3 (d) Expt 4 (SS316 with 0% TCP at 50 μm Layer Thickness)

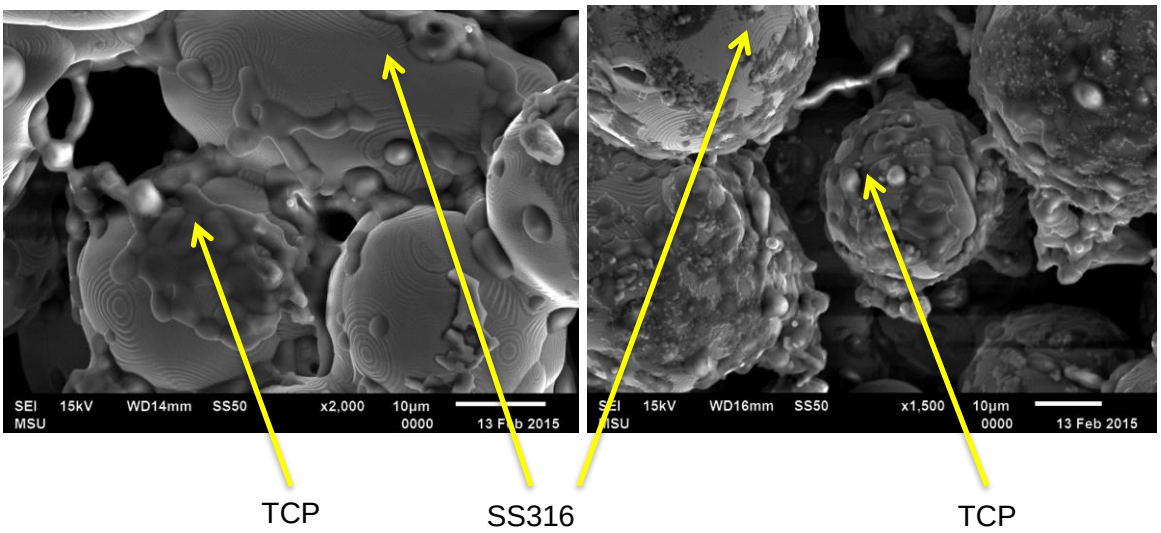

Fig. 7: SEM Images of the SS316-TCP biocomposite. (Left) – 80% SS316-20% TCP by volume, (Right) – 60% SS316-40%TCP by volume. Both are for 50 µm layer thickness, 2 Hour sintering at 1100 ^{0}C)

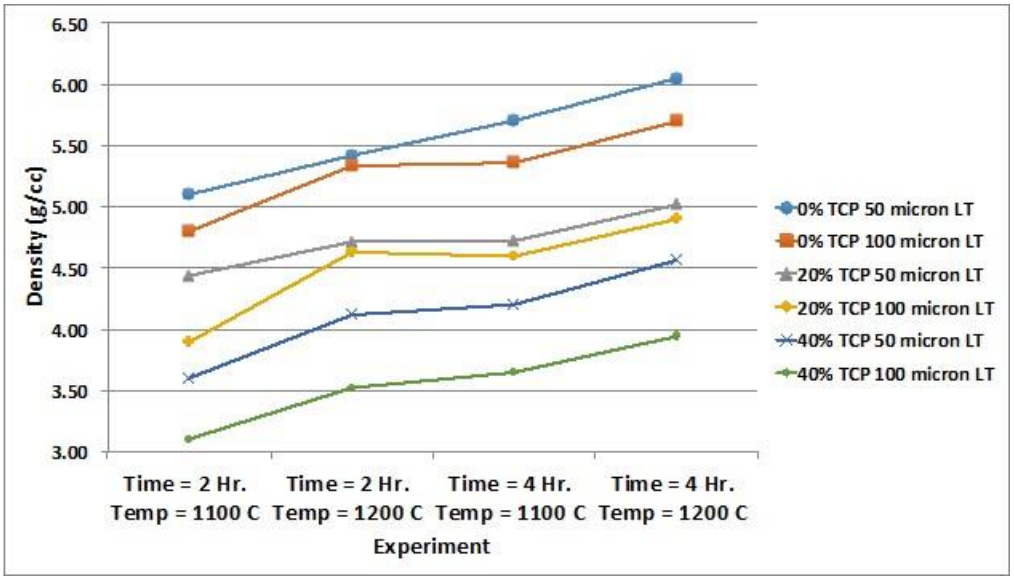

Fig. 8: Variation of densities in different experiments (LT = Layer Thickness)

Figure 6 and 7 show the different stages of sintering and the effect of different compositions. The experiment 1 (time = 2 hr and temp =1100 ^{0}C) has a very small neck to diameter ratio showing the onset of the sintering (initial phase). Comparison between experiments 1 and 2 and experiments 1 and 3 shows that temperature has a greater effect on sintering than the time. The pore size also decreases from an average of 20 µm in experiment 1 to 8 µm in experiment 4. The TCP forms a

kind of coating on the SS particles as can be seen in Fig. 7. The higher the volume fraction of TCP, the more it coats the SS particle and forms a layer on them.

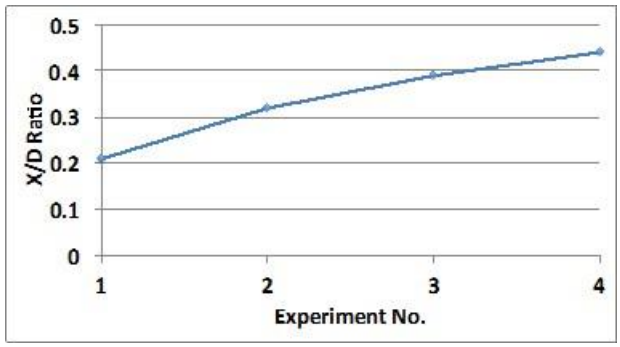

Fig. 8: Neck to diameter ratio for the different experiments for SS316 with 0% TCP samples

Compression testing

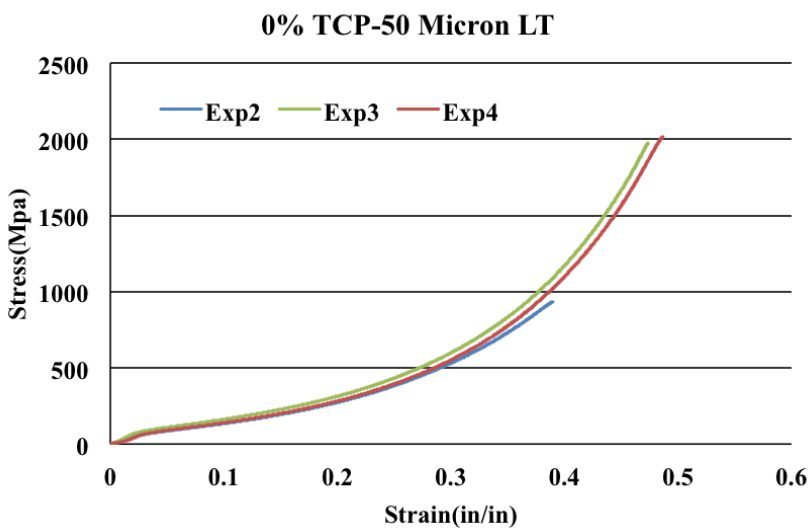

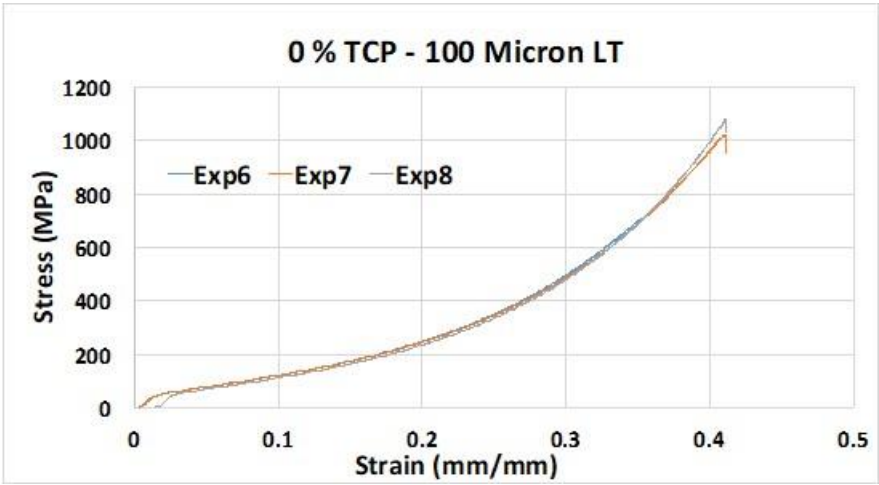

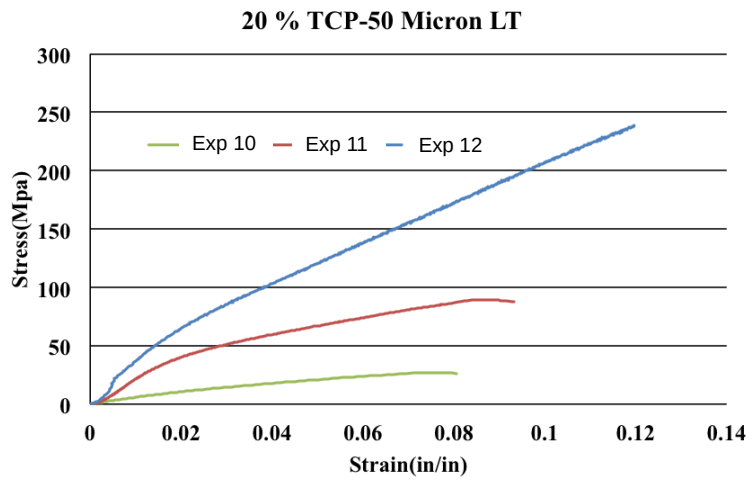
20 % TCP-50 Micron LT
Exp 10
Exp 11
Exp 12
Stress(Mpa)
Strain(in/in)
300
250
200
150
100
50
0
0
0.02
0.04
0.06
0.08
0.1
0.12
0.14

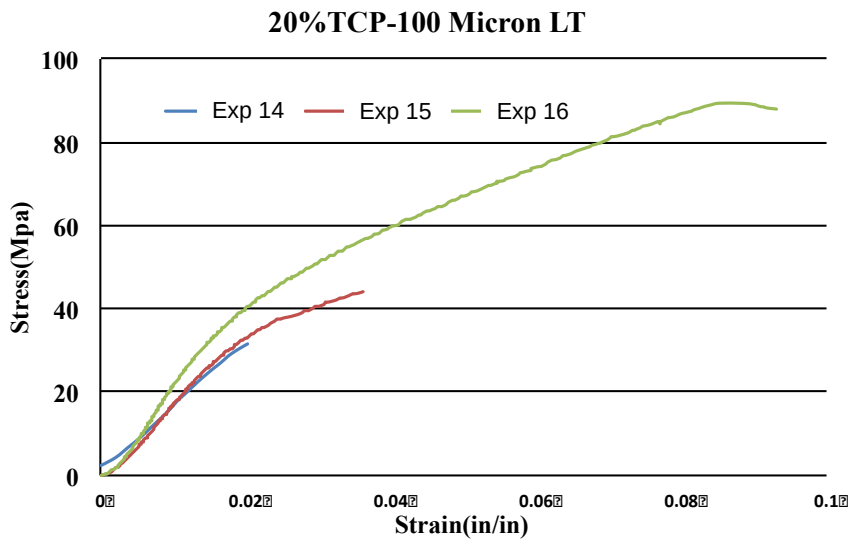
20%TCP-100 Micron LT
Exp 14
Exp 15
Exp 16
Stress(Mpa)
Strain(in/in)
100
80
60
40
20
0
0
0.02
0.04
0.06
0.08
0.1

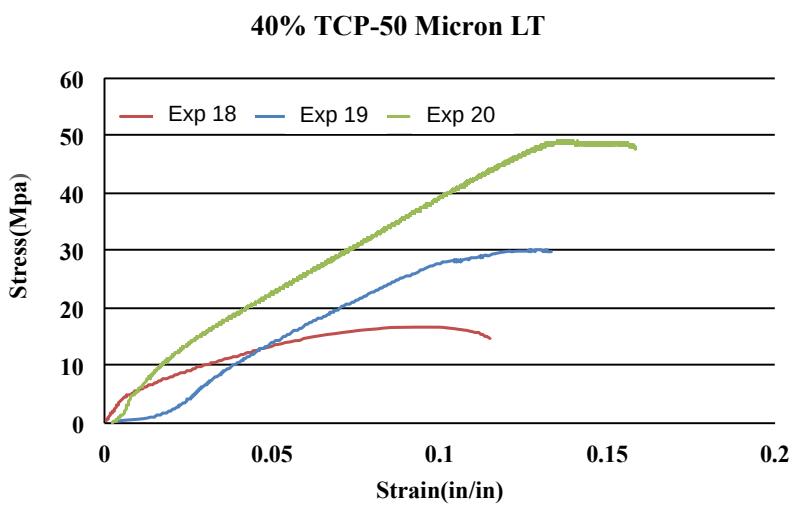
40% TCP-50 Micron LT
Exp 18
Exp 19
Exp 20
Stress(Mpa)
Strain(in/in)
60
50
40
30
20
10
0
0
0.05
0.1
0.15
0.2

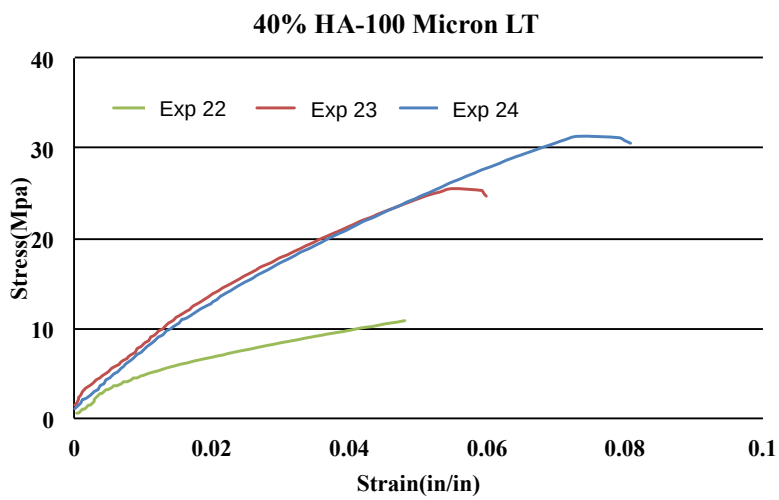

Fig. 9: Stress Strain Curves for the Various Experiements

Expt No.	% TCP	Layer Thickness (µm)	Sintering Time (Hrs)	Sintering Temp (^{0}C)	Elastic Modulus (GPa)	Ultimate Compressive Strength(Mpa)
1	0	50	2	1100	-	-
2	0	50	2	1200	83.4	978.2
3	0	50	4	1100	113.4	1742.2
4	0	50	4	1200	129.5	1987.7
5	0	100	2	1100	-	-
6	0	100	2	1200	78.4	803.8
7	0	100	4	1100	105.5	1033.6
8	0	100	4	1200	120.7	1076.6
9	20	50	2	1100	-	-
10	20	50	2	1200	12.1	26.9
11	20	50	4	1100	27.3	89.36
12	20	50	4	1200	32.4	238.16
13	20	100	2	1100	-	-
14	20	100	2	1200	13.2	21.3
15	20	100	4	1100	21.9	43.78
16	20	100	4	1200	29.8	89.39
17	40	50	2	1100	-	-
18	40	50	2	1200	9.2	16.7
19	40	50	4	1100	11.1	28.37
20	40	50	4	1200	13.6	48.8
21	40	100	2	1100	-	-
22	40	100	2	1200	8.3	10.9
23	40	100	4	1100	13.6	25.23
24	40	100	4	1200	15.7	31.7

Table 3: Results from the Compression Experiments. The blank spaces indicates that the samples crumbled immediately on compression

The compression tests show the following features:

a) 50 Micron Layer thicknesses have higher compressive strength than the 100-micron layer thickness for all material compositions.
b) The strength follows the same pattern as the densities and the neck – diameter ratios. The strength is higher for 4 hour 1100 ^{0}C than for 2 Hour 1200 ^{0}C sintering.
c) The samples were not sintered completely at 2 hours and 1100 ^{0}C and hence crumbled immediately on compression.
d) The compressive strength varied from a peak of 1987.7 MPa for certain settings to a low of 803.8 MPa for SS samples
e) The compressive strength of 20% TCP samples was higher for the same settings than the 40% TCP samples.
f) The Elastic modulus of both 20% and 40% TCP samples is within the range of cortical and cancellous bones (7-30 GPa).

Thus, there are a variety of bone implant and scaffold applications that are possible by a biocomposite manufactured by binder jet AM process. For some implant applications 20% TCP-80% SS biocomposite can be used, while for others a 40% TCP – 60% SS biocomposite can be used. The processing can be done differently to make sure that the materials have the required strength.

Conclusions

Scaffolds are 3D biocompatible structures that mimic the extracellular matrix properties (mechanical support, cellular activity and protein production) of bones and provide place for cell attachment and bone tissue formation. Their performance depends on chemistry, pore size, pore volume, and mechanical strength. Recently, additive manufacturing (AM) has been used as a means to produce these scaffolds. This paper explores a new biocomposite manufactured using Binder Jet AM process. SS and TCP are combined to form a composite and used in different volume fractions to produce parts with varying densities. Layer thickness, sintering time, and sintering temperature are varied to study the effect of process parameters on the microstructure, dimensions, and mechanical properties of the resulting structure. It was found that the resulting biocomposite can be tailored by varying the process to change its properties and mimic the properties of scaffolds in bone tissue applications.

The different compositions can be used to produce implants or scaffolds depending on their strength characteristics. 20% TCP biocomposite is more suitable for implant applications, while the 40% TCP biocomposite is more suited for scaffold applications.

Further work needs to be done to determine the biocompatibility and wear characteristics of these materials before can be a candidate for the biomedical applications.

References

1. Tarafder, S., 2013. Physicomechanical, In Vitro and in Vivo Performance of 3D Printed Doped Tricalcium Phosphate Scaffolds for Bone Tissue Engineering and Drug Delivery, Ph.D. *Dissertation,*

2. Butscher, A., Bohner, M., Hofmann, S., Gauckler, L., Müller, R., 2011, Structural and material approaches to bone tissue engineering in powder-based three-dimensional printing, *Acta Biomaterialia* 7, pp. 907–920.
3. Ahmadi, S. M., Yavari, S.A., Wauthle, R., Pouran, B., Schrooten, J., Weinans H., Zadpoor, A.A., 2015. Additively Manufactured Open-Cell Porous Biomaterials Made from Six Different Space-Filling Unit Cells: The Mechanical and Morphological Properties, *Materials*, 8, pp. 1871-1896; doi:10.3390/ma8041871.
4. Kolan, K., Thomas, A., Leu, M.C., Hilmas, G., 2015. In vitro assessment of laser sintered bioactive glass scaffolds with different pore geometries, *Rapid Prototyping Journal*, Vol. 21 Iss: 2, pp.152 – 158.
5. Bose, S., Vahabzadeh, S., Bandyopadhyay, A., 2013. Bone tissue engineering using 3D printing, *Materials today*, Volume 16, Issue 12, pp. 496–504.
6. Bose, S., Roy, M., Bandyopadhyay, A., 2012. Recent advances in bone tissue engineering scaffolds, *Trends in Biotechnology*, Volume 30, Issue 10, pp. 546–554.
7. Alvarez, K., Nakajima, H., 2009. Metallic Scaffolds for Bone Regeneration, *Materials*, 2, pp. 790-832; doi:10.3390/ma2030790.
8. MitraAsadi-Eydivand, MehranSolati-Hashjin, Farzad, A., 2016. Effect of technical parameters on porous structure and strength of 3D printed calcium sulfate prototypes, *Robotics and Computer-Integrated Manufacturing, 37*, pp. 57–67.
9. Cox, S.C., Thornby, J.A, Gibbons, G.J., Williams, M.A, Mallick, K.K, 2015. 3D printing of porous hydroxyapatite scaffolds intended for use in bone tissue engineering applications, *Materials Science and Engineering* C 47, pp. 237–247.
10. Standard Test Methods of Compression Testing of Metallic Materials at Room Temperature. *ASTM International, Designation: E9-09.*
11. Lou, T., Wang, X., Song, G., Gu, Z., Yang, Z., 2015. Structure and properties of PLLA/b-TCP nanocomposite scaffolds for bone tissue engineering, *J Mater Sci: Mater Med, pp.* 26-34.
12. Ashby, M.F, Evans, A.G., Fleck, N.A., Gibson, N.A., Hutchinson, J.W., Wadley, H.N.G., 2000. Metal Foams: A Design Guide, *Butterworth-Heinemann*
13. German, R., 1996. Sintering Theory and Practice, *Wiley-VCH*
14. Bartolo, P., Kruth, J., Silva, J., Levy, G., Malshe, A., Rajurkar, K., Mitsuishi, M., Ciurana, J., Leu, M., "Biomedical production of implants by additive electro-chemical and physical processes", CIRP Annals - Manufacturing Technology 61 (2012), 635-655